NON-LINEAR UNSTEADY WING THEORY

Part I

Quasi Two-Dimensional Behavior:
Airfoils and Slender Wings

J.E. McCune, Professor of
Aeronautics and Astronautics
Massachusetts Institute of Technology
Cambridge, MA 02139

June, 1987

NASA Grant NAG-1-658

Foreword

This document comprises a report of progress made in the initial phases of a long-term research effort aimed at understanding the unsteady interactive aerodynamics of large-amplitude wing motions and maneuvers. This part of the research was supported by NASA-Langley under Grant Nr. NAG-1-658. The work is being continued with support from other agencies.

Abstract

The initial phases of a study of the large-amplitude unsteady aerodynamics of wings in severe maneuver are reported. The research centers on vortex flows, their initiation at wing surfaces, their subsequent convection, and their interaction dynamically with wings and control surfaces. This report focuses on 2D and quasi-2D aspects of the problem and features the development of an exact non-linear unsteady airfoil theory as well as a new approach to the cross-flow problem for slender wing applications including leading-edge separation. The effective use of interactive on-line computing in quantifying and visualizing the non-steady effects of severe maneuver is demonstrated. The effects of viscosity in establishing and limiting the size of vortex cores is also being investigated in a companion effort not reported here.

In the first part of this study, analysis of 2D unsteady airfoil behavior was developed along lines analogous to classical theory, except that no linearizing assumptions were admitted. Successful use of certain convective characteristic variables [1] has led to a viable non-linear wing theory for unsteady flow past airfoils in violent motion. The theory reproduces classical results in the limit of very low amplitudes. This part of the research sets the stage for a similar study of the slender wing cross-flow problem. [2]

The new non-linear airfoil theory has been implemented on the computer. Interactive computational work is now possible, in which a "maneuver" can be initiated (i.e., input) and its effects observed and analyzed immediately (i.e., on-line). Typical results from these studies are discussed in the report (Section II) and, where possible, compared with classical linear theory. The effects of certain severe maneuvers are illustrated.

A video tape of representative interactive computational results is also available and can be obtained from the author on request.

I. Non-Linear Unsteady 2D Airfoil Theory and the Quasi-2D Cross-Flow Problem

The goals of this research do not actually include, per se, the development of non-linear unsteady 2D airfoil theory as it might be applied, for example, to large aspect ratio wings in violent maneuver. Rather, we are interested here in developing the tools with which the non-linear unsteady aerodynamics of slender wings, including deltas, can be studied. However, in the process of putting these tools in place, particularly for the cross-flow problem, it is useful and natural to study the 2D unsteady airfoil case.

A. Comparisons

A major feature of classical linearized unsteady wing theory (2D or 3D) is the introduction of crucial simplifications regarding the wake. Recognizing even in 2D airfoil treatments that vorticity (incremental circulation) must be shed into the wake behind a host body on which the bound circulation varies in time, the classical description approximates the spatial location and motion of that vorticity. One assumes namely that all shed vorticity lies in the plane of the incoming undisturbed flow vector passing through the midchord location of the corresponding airfoil or wing mean camber line at mid-span. Moreover, in the linear model each increment of circulation is assumed to be "convected" approximately by the undisturbed free stream speed, U_∞, say. The latter assumption, of course, is the linearized version of the constraint that the vorticity in the wake is "free", i.e., supports no force.

In reality the wake vorticity moves at a speed and direction determined not only by the free stream but also by the "induced" velocities associated with both the bound vorticity on the wing and the neighboring "free" vorticity in the wake or wakes. The result in the 2D airfoil case is that even at very low amplitudes of airfoil motion in pitch or plunging there is a net displacement of the wake relative to the plane of the wing or airfoil. In addition, there is coagulation of the vorticity, distortion of the wake and, eventually, possible roll-up into cores sometimes resembling spirals.[3] (See Figure I.1.)

Such features of the wake motion not included in linear theory can have several important effects. One of the more obvious is the introduction of additional "bound" vorticity on the wing needed to cancel out at the wing the "induced" normal velocities associated with the wake or wakes when the actual positions of the vortex elements is treated correctly. (See Figures I.2 and I.3.) Wake deformation affects directly both the bound vorticity and the Bernoulli "$\partial\phi/\partial t$" term needed to determine the wing loading in unsteady motion or maneuver.

Also important, as it turns out, is the fact that the topside-to-bottomside mean velocity at the airfoil is modified (relative to the linear version) whenever there is a net displacement of the wake. The net result is a further change in the airfoil loading. Both magnitude and phase are modified relative to the predictions of the linear model.

An interesting feature of the non-linear 2D airfoil work that follows is that for simple "benchmark" examples such as pure pitching or pure plunging, the amplitude threshold of important non-linear effects can be determined, most prominently as a function of the reduced frequency. No particular emphasis on these thresholds is contained in this report; we content ourselves with noting that they are very low even at relatively modest reduced frequencies. (See Section II.)

An additional advantage of studying this aspect of the overall problem has also emerged recently. Work on the non-linear aerodynamics of 2D airfoils of other authors, notably that of Mook, et. al. [4], has become available and provides us with a rich and convenient source of comparisons against which both fundamentals and accuracy of computation can be checked.

B. Non-Linear Treatment of the Wake

In the classical linear theory, having approximated the location and motion of the wake vorticity, the next step is to devise a means of determining the instantaneous magnitude of that vorticity, γ_w, everywhere in the wake. Representative of this approach is the well-known Wagner integral equation for γ_w [5] applicable for example to a plunging and pitching "flat plate" airfoil

$$\underset{\text{(known)}}{\Gamma_0(t)} = -\int_{\frac{c}{2}}^{x_{end}(t)} dx \underset{\text{(unknown)}}{\gamma_w(x-U_\infty t)} \sqrt{\frac{x+\frac{c}{2}}{x-\frac{c}{2}}} \qquad \text{(I.B.1)}$$

where $\Gamma_0(t)$ is the known instantaneous Kutta value of circulation that would be appropriate to satisfy the boundary condition at the plate in the absence of any wake. In the above, c/2 is the airfoil semi-chord, U_∞ is the free stream speed, and $x_{end}(t)$ is the downstream location of wake end, according to the linearized model. Thus, by linear theory, if $v_0(x,t)$ is the required normal velocity at the plate

$$v_0(x,t) \doteq \dot{h}(t) - x\,\dot{\alpha}(t) - U_\infty\,\alpha(t) \qquad \text{(I.B.2)}$$

and, if the Kutta condition is applied in the same spirit,

$$\Gamma_0(t) = -2\int_{-\frac{c}{2}}^{\frac{c}{2}} dx\; v_0(x,t) \sqrt{\frac{\frac{c}{2}+x}{\frac{c}{2}-x}} \qquad \text{(I.B.3)}$$

Here, h(t) is the vertical plunging location of the plate and $\alpha(t)$ is the angle of attack. Thus, if $Y_c(x,t)$ is the camber line of the plate, $Y_c = h(t) - x\tan\alpha \doteq h(t) - x\alpha$ where x is measured from midchord.

Many authors [5], [6], [7] have exploited this approach in linear theory to determine the wake vorticity for such classical examples as the steady-state low-amplitude oscillation of the plate in pitch or plunge (including possible flutter) and the "gust" problems.

Once the wake vorticity is known, the loading, lift, and moment can be calculated. This procedure uses the fact that the wake alters the apparent upwash at the airfoil so that additional bound vorticity on the airfoil is required to cancel out the wake effect. (See Figure I.3.) The net result is an alteration of the loading, lift and moment, both in phase and magnitude.

Early in the present investigation we were able to show [8] that the Wagner integral equation, as such, can be generalized to the non-linear case with arbitrary amplitude (always applying, however, the Kutta condition) for a flat plate or any Joukowski airfoil, even including wake displacement and roll-up exactly.

In the framework of the interactive computer studies we have developed, (see also Section II) the solution of the generalized Wagner is relatively straightforward. As the history of the wake formation and the associated airfoil motion, loading, and moment are developed at each time step and displayed on the screen, the incremental value of circulation that must be shed into the wake in order to maintain the Kutta condition (for example) is recorded. Then, as time proceeds, and using the methods proposed in Ref. [1], the instantaneous location of that incremental circulation is computed exactly and charted. The net result is an exact, non-linear (and virtually automatic) mapping at any instant of the wake intensity and shape. No CFD-type grid is required at any time.

Once the wake structure is available, the non-linear theory proceeds by analogy with the linear theory. For the flat plate and Joukowski airfoils, in fact, the generalization to arbitrary amplitude proceeds with surprising convenience. The exact boundary condition, representing the generalization of Equation (I.B.2) is, for example,

$$v_0(\hat{x},t) = \dot{h}(t) - \hat{x}\,\frac{\dot{\alpha}}{\cos\alpha(t)} - u^{\pm}\tan\alpha(t) \qquad \text{(I.B.4)}$$

where $\hat{x}$ is measured from midchord but along the actual plate surface, i.e., $\hat{x} = x/\cos\alpha$. (See Figure I.2.)

Using the theory of conjugate functions in the "circle-plane" obtained by an instantaneous Joukowski transformation from the physical plane, one is able to solve the problem for the airfoil loading almost precisely as in linear theory. Results for violent airfoil motion and maneuver* are then readily obtained, some of which are discussed in Section II.

For completeness, we record in Section I.C some of the key relationships that make the non-linear theory possible. In Section I.D a brief discussion of how the 2D theory is to be modified for the treatment of the slender wing 2D "cross-flow" problem is included.

---

*The results described above apply, of course, only if the instantaneous Kutta condition is reasonable. Effects of separation, leading-edge and otherwise, are being investigated and are reported elsewhere.

C. Exact (Non-Linear) Updates of Linear Theory for an Oscillating Plate

We need to solve $\nabla^2\phi = 0$ with appropriate boundary conditions for this problem without linearizing.

The exact boundary condition for an oscillating plate in pitch and plunge is given in (I.B.4). In terms of the instantaneous normal component, $\hat{v}$, at the plate, where

$$\hat{v} = v \cos\alpha + u \sin\alpha$$
$$\hat{u} = -v \sin\alpha + u \cos\alpha$$

we find without approximation

$$\hat{v}\Big|_{\text{plate}} = \dot{h} \cos\alpha(t) - \hat{x}\,\dot{\alpha} \qquad \text{(I.C.1)}$$

Here, $\hat{x}$ and $\hat{y}$ are the instantaneous cartesian coordinates centered on and parallel to and normal to the plate, respectively. (See Figure I.2.) Thus,

$$\hat{x} = x \cos\alpha - (y-h) \sin\alpha$$
$$\hat{y} = (y-h) \cos\alpha + x \sin\alpha \qquad \text{(I.C.1a)}$$

so that on the plate, where $\hat{y} = 0$, $y-h = -x \tan\alpha$, and $\hat{x} = (x/\cos\alpha)$. Note that for steady flow at any angle of attack, $\hat{v} = 0$ as required.

To solve this potential problem it is convenient to use an instantaneous conformal mapping such that, if $\zeta = x + iy$ and $Z = X + iY = Re^{i\theta}$, then

$$\zeta = Z + \frac{R_0^2\, e^{-2i\alpha(t)}}{Z} + ih(t)$$

where $2R_0 = c/2$. Thus, on a circle $Z = R_0 e^{i\theta}$ in the "Z-plane"

$$\hat{\zeta}\Big|_{\text{plate}} = (\hat{x} + i\hat{y})\Big|_{\text{plate}} \equiv e^{-i\alpha}(\zeta - ih)\Big|_{\text{plate}} = 2R_0 \cos(\theta+\alpha) \qquad \text{(I.C.2)}$$

Matching real and imaginary parts, one finds

$$\text{Re}(e^{i\alpha}(\zeta - ih)) \equiv \hat{x} = 2R_0 \cos(\theta+\alpha) \equiv c/2 \cos(\theta+\alpha)$$
$$\text{Im}(e^{i\alpha}(\zeta - ih)) \equiv \hat{y} = 0 \qquad \text{(I.C.3)}$$

so that this particular circle in the Z-plane maps the plate precisely.

Completing the conformal map one identifies the complex potentials in the ζ- and Z-planes, and finds the relationships between the corresponding velocity components. In particular, on the plate and circle surfaces

$$\begin{aligned} v_R\big|_{\text{circle}} &= 2\hat{v}\big|_{\text{plate}} \sin\beta \\ v_\theta\big|_{\text{circle}} &= -2\hat{u}\big|_{\text{plate}} \sin\beta \end{aligned} \qquad \text{(I.C.4)}$$

where

$$\beta \equiv \theta + \alpha \qquad \text{(I.C.5)}$$

In the circle plane the mathematical problem is relatively easy to solve using the theory of conjugate functions. When the Kutta condition at the trailing edge is assumed, the results are typified by

$$\hat{u}\big|_{\text{plate}} = U_\infty \cos\alpha + \frac{U_\infty \sin\alpha(1-\cos\beta)}{\sin\beta} - \frac{L_c^K(\beta)\{2\sin\tau\,\hat{\hat{v}}\}}{2\sin\beta} + \hat{u}_w \qquad \text{(I.C.6)}$$

where $\beta \equiv \theta + \alpha$ and $\hat{u}\big|_{\text{plate}}$ is the component of velocity parallel to the plate at its surface. Since $\hat{x} = c/2\cos\beta$ from (I.C.3) the upper plate surface corresponds to $(0 \le \beta \le \pi)$, while the lower surface is specified by $(\pi \le \beta \le 2\pi)$. In the above, the third term involves the conjugate function operator "L_c^K", with $2\sin\tau\,\hat{\hat{v}}(\tau)$ as operand, "A". $\hat{u}_w$ and $\hat{\hat{v}}$ will be defined presently. With the Kutta condition applied, $L_c^K(\beta)\{A\}$ is given by

$$L_c^K(\beta)\{A(\tau)\} \equiv L_{CK}^{\text{even in }\beta}(\beta)\{A\} + L_{CK}^{\text{odd in }\beta}(\beta)\{A\} \qquad \text{(I.C.7)}$$

where

$$L_{CK}^{\text{even}}(\beta)\{A(\tau)\} \equiv \frac{+(1-\cos\beta)}{\pi} P\int_0^\pi \frac{d\tau A^{\text{odd}}(\tau)}{\sin\tau} \frac{1+\cos\tau}{\cos\tau-\cos\beta} \qquad \text{(I.C.7a)}$$

$$L_{CK}^{\text{odd}}(\beta)\{A(\tau)\} \equiv +\frac{1}{\pi} P\int_0^\pi d\tau\, A^{\text{even}}(\tau) \frac{\sin\beta}{\cos\tau-\cos\beta} \qquad \text{(I.C.7b)}$$

where $A(\tau) = A^{\text{odd in }\tau}(\tau) + A^{\text{even in }\tau}(\tau)$.

The result in (I.C.6) has necessarily been adjusted to include the effects of the wake, as suggested in Figure I.3, just as in Wagner's theory [5]. For example, $\hat{u}_w$ in (I.C.6) is the parallel velocity component to be calculated at the plate surface due to the wake. Moreover,

$$\hat{\hat{v}} \equiv \hat{v}\Big|_{\text{plate}}(\beta) - \hat{v}_w(\beta) \qquad \text{(I.C.8)}$$

where $\hat{v}\Big|_{\text{plate}}$ is given in (I.C.1) and $\hat{v}_w$ is the normal component of velocity due to the wake. Both $\hat{u}_w(\beta)$ and $\hat{v}_w(\beta)$ are obtained via the Biot-Savart Law, once the exact non-linear wake structure has been obtained.

The parallel induced velocity $\hat{u}_w$ at the plate, of course, has no discontinuity. Thus, if $-\Delta\hat{u} \equiv \gamma \equiv -(\hat{u}_{top} - \hat{u}_{bottom})$ and $\langle\hat{u}\rangle \equiv (\hat{u}_{top}+\hat{u}_{bottom})/2$ then

$$\Delta\hat{u} = -\gamma = 2U_\infty \sin\alpha \left(\frac{1-\cos\beta}{\sin\beta}\right) - \frac{L_{CK}^{even}(\beta)\{A^{odd}\}}{\sin\beta} \qquad \text{(I.C.9)}$$

while

$$\langle\hat{u}\rangle = U_\infty\cos\alpha + \hat{u}_w(\beta) - \frac{L_{CK}^{odd}(\beta)\{A^{even}\}}{2\sin\beta} \qquad \text{(I.C.10)}$$

where, again, $A = 2\sin\tau\left(\hat{v}\Big|_{\text{plate}}(\tau) - \hat{v}_w(\tau)\right)$.

For the flat plate case, no matter the amplitude of the unsteady motion, L_{CK}^{odd} vanishes since $A(\tau)$ is pure odd. Thus,

$$\langle\hat{u}\rangle_{\text{flat plate}} = U_\infty\cos\alpha + \hat{u}_w(\beta) \qquad \text{(I.C.10a)}$$

Note that $\hat{u}_w$, being due to the wake, will vary, along with other effects, according as a net displacement of the wake from the plane of the wing does or does not develop.

The results in (I.C.9) and (I.C.10) are part of what is needed to calculate the airfoil loading, $p] \equiv (p_{bottom}-p_{top})$. In fact, from the Bernoulli equation

$$p] = +\rho_\infty\left[\langle\underset{\sim}{q}\rangle\cdot\Delta\underset{\sim}{q} + \Delta\left(\frac{\partial\phi}{\partial t}\right)\right]$$

where ϕ is the velocity potential and $\underset{\sim}{q}$ is the fluid velocity vector. Also, $\langle(\,)\rangle \equiv \tfrac{1}{2}\left((\,)_{top} + (\,)_{bottom}\right)$ and $\Delta(\,) \equiv (\,)_{top}-(\,)_{bottom}$. Since $\Delta\hat{v} = 0$ in this case, $\Delta\underset{\sim}{q}\cdot\langle\underset{\sim}{q}\rangle = \langle\hat{u}\rangle\Delta\hat{u}$, so that the plate loading becomes

$$p] = \rho_\infty\left[\langle\hat{u}\rangle\,\Delta\,\hat{u} + \Delta\left(\frac{\partial\phi}{\partial t}\right)\right] \qquad \text{(I.C.11)}$$

The "$\Delta\left(\frac{\partial\phi}{\partial t}\right)$" term, related to "apparent mass" effects, can also be calculated exactly. Letting

$$\Phi(\hat{x},\hat{y},t) \equiv \phi\ (x,y,t), \tag{I.C.12}$$

where $\hat{x}(x,y,t)$ and $\hat{y}(x,y,t)$ are defined in (I.C.1a), the result is [8]

$$\Delta\left(\frac{\partial\phi}{\partial t}\right) = \frac{\partial}{\partial t}\Big|_{\text{fixed } \hat{x},\hat{y}} \Delta\Phi\ (\hat{x},\hat{y},t) + \Delta\hat{u}\ \dot{h}\ \sin\alpha(t) \tag{I.C.13}$$

But $\Delta\Phi$ is easily available given $\Delta\hat{u}$ as given in (I.C.9); in fact,

$$\Delta\Phi = c/2 \int_{\beta}^{\pi} d\beta\ \sin\beta\ \Delta\hat{u}\ ,$$

so that

$$\Delta\Phi_t = c/2 \int_{\beta}^{\pi} d\beta\ \sin\beta\ (\Delta\hat{u})_t \tag{I.C.14}$$

where, again, $\cos\beta = \frac{\hat{x}}{c/2}$ so that $\sin\beta = \left(1 - \frac{\hat{x}^2}{(c/2)^2}\right)^{\frac{1}{2}}$ and $d\hat{x} = -\frac{c}{2}\sin\beta\, d\beta$.

Given the loading expressed in this fashion, the instantaneous lift and moment of the plate are calculated readily from

$$\left(\frac{\text{lift}}{\text{unit span}}\right) \quad L(t) = \frac{c/2}{\cos\alpha} \int_{0}^{\pi} d\beta\ \sin\beta\ p] \tag{I.C.15}$$

and

$$\left(\frac{\text{moment}}{\text{unit span}}\right) \quad M_0(t) = (c/2)^2 \int_{0}^{\pi} d\beta\ \sin\beta\ \cos\beta\ p] \tag{I.C.16}$$

where "M_0" is measured from mid-chord and is positive nose down.

Note that the expression in (I.C.15) is adjusted for the "leading edge force" in the classical manner. This, of course, means that not only have we applied a Kutta condition at the trailing edge but that we are also omitting for the moment any effects of leading-edge separation of the 2D airfoil type.

The multiple integrals in (I.C.15) and (I.C.16) can all be reduced in the manner of Munk [9], so that, at most, only a single quadrature over the airfoil chord is required at any instant to determine L(t) and $M_0(t)$. (See Ref. [8] for details.) Thus, for the "flat plate airfoil",

$$L(t) = \rho_\infty \frac{c}{2} \left\{ \int_0^\pi d\beta \left(U_\infty + \dot{h} \tan\alpha + \frac{\hat{u}_w}{\cos\alpha} \right) \left(2U_\infty \sin\alpha (1-\cos\beta) - L_{CK}^{even} \right) \right.$$
$$\left. + \frac{c}{2} \int_0^\pi \frac{(1-\cos\beta)}{\cos\alpha} \frac{\partial}{\partial t} \left(2U_\infty \sin\alpha\,(1-\cos\beta) - L_{CK}^{even} \right) d\beta \right\} \qquad \text{(I.C.17)}$$

whereas

$$M_0(t) = \rho_\infty \left(\frac{c}{2}\right)^2 \left\{ \int_0^\pi d\beta \cos\alpha \cos\beta \left(U_\infty + \dot{h} \tan\alpha + \frac{\hat{u}_w}{\cos\alpha} \right) \left(2U_\infty \sin\alpha (1-\cos\beta) - L_{CK}^{even} \right) \right.$$
$$\left. + \frac{c}{8} \int_0^\pi (1-\cos 2\beta) d\beta \frac{\partial}{\partial t} \left(2U_\infty \sin\alpha\,(1-\cos\beta) - L_{CK}^{even} \right) \right\} \qquad \text{(I.C.18)}$$

Note that the final "$\partial\phi/\partial t$" terms in (I.C.17) and (I.C.18) have each been integrated once by parts. Equation (I.C.17) can also be obtained by applying the principle of conservation of impulse.

These exact (non-linear) results, together with the non-linear version of the Wagner integral equation mentioned above, have been used by Scott [8] to obtain the non-linear unsteady results discussed in Section II. Scott's lift and moment results, and that part of his NLWAKE code as of this writing, are based on Equation (I.C.17) and (I.C.18).

However, we have recently recognized that these equations, as written, are not as convenient for computational purposes as they could be. For example, in the above expression for L (t) the term

$$-\rho_\infty \frac{c}{2} \int_0^\pi d\beta\, (U_\infty + \dot{h} \tan\alpha)\, L_{CK}^{even}(\beta) \equiv -\rho_\infty (U_\infty + \dot{h} \tan\alpha)\, \Gamma_1 \qquad \text{(I.C.19)}$$

is a wake-effect contribution where Γ_1 is defined as in [6] (see Section II.a.). We will show in Section III, however, that this contribution is <u>almost exactly cancelled</u> by the term

$$\frac{\rho_\infty}{\cos\alpha} \left(\frac{c}{2}\right)^2 \frac{d}{dt} \int_0^\pi \cos\beta\, d\beta\, L_{CK}^{even}(\beta) \qquad \text{(I.C.20)}$$

in the second integral of (I.C.17). The difference between the two is the non-linear version of the "L_2" wake-effect lift formulated by von Kármán and Sears.[6]

Computationally this means that one is attempting to calculate a small residual lag- or lead-effect by taking the difference between two much larger quantities, a situation obviously to be avoided from the numerical point of view. (See Section II.B.)

The procedure is vastly improved in this respect by reformulating the wake-induced terms in (I.C.17) (for example), in terms of integrals over the wake. An account of how this can be carried out is given in Section III.

D. The Cross-Flow Problem with Two Wakes

In this section we discuss briefly the development of the quasi-two-dimensional cross-flow problem appropriate for application to a slender (low $\mathcal{AR}$) delta wing. We content ourselves with a "flat plate" wing under symmetrical loading and use the time-analogy approach of Munk and Jones, because we have a limited objective here. In particular, we wish to demonstrate the necessity of vortex wakes "emanating" from each edge of the wing (in the cross-plane view) provided one assumes a Kutta condition (i.e., smooth edge flow) to apply at those edges. (Compare Figures I.4 and I.5.) In the linear version, one can approximate the location of these wakes, and the cross-plane motion of the vorticity within them, in a manner analogous to the classical linear airfoil theory of Section I.B. An integral equation for the vorticity strength within the wakes results which plays a role for this problem similar to that of the Wagner equation in the linear airfoil analysis. The non-linear treatment of the same problem can then build on this approach, with the linear theory providing a "benchmark" as before. (Compare Sections I.B and I.C.)

In this simplified model, as illustrated in Figures I.4 and I.5, the wing trace representing the penetration of the flat delta wing moving at speed U_∞ through a fixed reference cross-plane (x,y) is a straight line, the "span" of which appears to grow in time. Moreover, if the flat delta has an angle of attack α, the trace through the fixed plane moves "down" (to the left, in Figure I.4) at speed $U_\infty \tan\alpha \triangleq U_\infty \alpha$. If we now fix our attention on a cross-plane fixed in the delta wing at some chordwise station z, this plane moves at speed U_∞ relative to the previous one and has a wing trace whose span is proportional to z if z is measured from the vertex of the delta. Moreover, in this fixed cross-plane there is an apparent wind (from the left, in Figure I.4) of magnitude $U_\infty \tan\alpha \triangleq U_\infty \alpha$.

Note that in Figures I.4 and I.5 "z" is out of the paper and the triad (x,y,z) is right-handed. The orientation of the coordinates was chosen to point up the analogy with a flat plate "airfoil" at 90° angle of attack, for eventual reference to the results of Sections I.C and II.

The linear version in the completely inviscid limit ($Re \equiv \infty$) of the cross-flow problems [2], [9], [10] includes no wake at all and thus cannot satisfy a Kutta condition at the edges. (Recall that according to the Kelvin theorem there can be no net circulation in any cross-flow plane.) In fact the flow solution in that case is represented by

$$u\Big|_{\text{plate}} = 0 \qquad \text{(normal component)}$$

$$v\Big|_{\text{plate}} = (-U_\infty \alpha) \tan\theta \qquad \text{(parallel component)} \tag{I.D.1}$$

where $y = \frac{b}{2} \sin\theta$. Thus, the flow in this limit is singular at the wing edges, since

$$\cos\theta = \sqrt{1 - \frac{y^2}{(b/2)^2}}$$

At any finite Re such singularities, of course, are unrealistic. At very large but finite Re we expect a smooth flow and postulate a Kutta condition at each edge.

To smooth this flow and apply such a Kutta condition, one requires two "wakes" of vortices (as viewed in the cross-plane) above the wing trace [11], [12], [13], [14].* (See Figure I.5.) In the linear case, and for the spanwise symmetry assumed here, one can locate the traces of these vortices. In complex variable notation we find $\zeta_v = h + is(h)$ at any z, where for steady flow at small α, (Fig. I.6)

$$h = \alpha(z - z_e), \tag{I.D.2a}$$

and

$$s(h) = \frac{b(z)}{2} - \frac{h(b/2)}{\alpha z}\{1-f\}. \tag{I.D.2b}$$

Here, b/2 is the local semi-span and h is the apparent height at z above the wing of the vortex element which "emanated" from the wing edge at the upstream chordwise station z_e. "s(h)" is then the spanwise location from midspan of the same element. Note that $b/2 = (\cot\Lambda)z$ where Λ is the wing sweep angle. The fraction f, $f < 1$, allows for a certain spanwise convection, $U_\infty \alpha f$, of the vortices. The companion (starboard side) wake is located at $\zeta_v^* = h - is(h)$. Note that, at any z, h varies from 0 to αz, and at $h = 0$, $s = b/2$. (See Figure I.6.)

But one may ask: why a pair of "wakes", or wake traces? We note that at any given z, for example, two point vortices above the wing trace would suffice by themselves to smooth the flow if their strengths were chosen properly for the given location, so one might consider that possibility. However, at the chordwise station immediately downstream, generally of different span, these two vortices, being free, will have convected to a new relative location above the new wing

*This phenomenon is often referred to as leading edge separation in the slender-wing literature.

We can then write

$$v\Big|_{\text{plate}} = (-U_\infty \alpha)\tan\theta + v_w\Big|_{\text{plate}}$$

$$- \frac{\tan\theta}{2\pi} \int_0^{\alpha z} dh\ \Gamma'(h)\ \mathrm{Re}\left\{ \frac{1}{\pi}\, P\!\int_{-\frac{\pi}{2}}^{\frac{\pi}{2}} \frac{d\tau\ \cos\tau}{\cos\tau - \cos\theta^*} \left\{ \frac{1}{b/2\ \sin\tau + i\zeta_v(h)} - \frac{1}{b/2\ \sin\tau + i\zeta_v^*(h)} \right\} \right\} \qquad \text{(I.D.7)}$$

The $v_w\Big|_{\text{plate}}$ term in I.D.7 is not singular enough to cancel the $\tan\theta$ singularity of the first term. It remains for the final integral term to be adjusted, by choice of $\Gamma(h)$, so as to smooth the flow and satisfy the Kutta conditions. One requires namely that the sum of the coefficients of $\tan\theta$ vanish in the limit $\theta \to \pm \pi/2$.

But in that limit, as $\cos\theta \to 0$, the inner integral in the final term of (I.D.7) can be carried out handily. The result is

$$\frac{1}{\pi} \int_{-\frac{\pi}{2}}^{\frac{\pi}{2}} d\tau \left\{ \frac{1}{b/2\ \sin\tau + i\zeta_v} - \frac{1}{b/2\ \sin\tau + i\zeta_v^*} \right\}$$

$$= \frac{1}{\sqrt{(i\zeta_v)^2 - (b^2/4)}} - \frac{1}{\sqrt{(i\zeta_v^*)^2 - (b^2/4)}} \qquad \text{(I.D.8)}$$

where the square roots are defined in the sense of complex variables and require determining the correct branch. Note that as $h \to 0$, where the wakes approach the wing at its edges, $i\zeta_v \to -b/2$ while $i\zeta_v^* \to +b/2$.

Satisfying the Kutta condition then requires

$$2\pi\, U_\infty \alpha = -\mathrm{Re} \int_0^{\alpha z} dh\ \Gamma'(h) \left\{ \frac{1}{\sqrt{(i\zeta_v)^2 - (b^2/4)}} - \frac{1}{\sqrt{(i\zeta_v^*)^2 - (b^2/4)}} \right\} \qquad \text{(I.D.9)}$$

This is an integral equation for the distribution of circulation element, $d\Gamma(h)$,

along the two symmetrical wakes. It will be noted that it bears a very close resemblance to the Wagner integral equation of classical airfoil theory (compare Sections I.B and I.C) as well as to the non-linear version of that equation obtained by Scott [8].

The non-linear unsteady version of (I.D.9) is actually the same, except that the explicit approximation (I.D.2) for the shape of the wake traces has to be dropped and the ζ_v remain to be found self consistently. As explained in Section I.C and in greater detail in Ref. [8], this replacement amounts to devising a scheme of mapping out the wake as time (and/or z/U_∞) progresses. This is precisely what Scott's codes [8] do for us, using the exact non-linear characteristic variables proposed in Ref. [1]. Thus, in illustrating in the next Section the results of his successful interactive treatment of the non-linear unsteady airfoil problem (albeit, with only one wake), we have set the stage for a similar application of the interactive method to the quasi-two-dimensional cross-flow problem in the non-linear, unsteady case, including two wakes. This work, to be used to help determine the unsteady aerodynamics of slender wings in severe maneuver, is being carried out in the extension of our work beyond the present NASA Grant. It is to be expected, of course, that relative to the linear theory the actual wakes will distort and very likely roll-up in most situations. In such cases the full theory may eventually emulate the models of Adams, Edwards, Cheng, Brown and Michael. [11], [12], [13], [14]. Results of this part of our study are to be reported elsewhere.

II. Typical Results: Non-Linear 2D Airfoil Behavior

A. Basic Method of Determining Wake-Effect Terms

The non-linear version of Eq. I.B.1 is [1], [8]

$$\underset{\text{(known)}}{-\Gamma_0(t)} = \text{Real Part}\left(-\int_t^0 d\lambda \ \frac{d\Gamma_w(\lambda)}{d\lambda} \sqrt{\frac{a(\lambda,t)+1}{a(\lambda,t)-1}}\ \right) \tag{II.1}$$

where $a(\lambda,t) = \frac{2}{c} e^{i\alpha(t)} \zeta_v(\lambda,t)$ is a complex function of time and the convection variable, λ. [1] Here, $\zeta_v = X_v + iY_v$ is the complex location of each wake vortex element of circulation $d\Gamma_w(\lambda)$. λ satisfies $\partial\lambda/\partial t + \langle q \rangle \cdot \nabla\lambda = 0$ at the wake and equals t at the trailing edge. Note that Γ_w, λ, and t are real. At any t, $a(\lambda=t,t)=a(t,t)=1$ representing a vortex element just leaving the trailing edge of the airfoil, so Eq. (II.1) is singular there. On the basis of this, Scott [8] has developed a code, NLWAKE, which automatically and efficiently determines the unknown circulation elements $d\Gamma_w(\lambda)$ for any given $\Gamma_0(t)$. Equation (II.1) is solved under the constraint, following from Kelvin's Theorem, that

$$\Gamma_{Bound}(t) \equiv \Gamma_0(t) + \Gamma_1(t) = -\Gamma_{wake}(t) \tag{II.2}$$

Note that the total wake circulation $\Gamma_{wake}(t)$ is

$$\Gamma_{wake}(t) = -\int_t^0 \frac{d\Gamma_w(\lambda)}{d\lambda} d\lambda \tag{II.3}$$

so that $\Gamma_1(t)$, defined by (II.2), is just

$$\Gamma_1(t) = \text{Real Part}\left(-\int_t^0 d\lambda \ \frac{d\Gamma_w}{d\lambda} \left(\sqrt{\frac{a+1}{a-1}} - 1\right)\right) \tag{II.4}$$

Once the $d\Gamma_w(\lambda)$ are determined we have all the information needed to calculate the wake terms in Eqns. (I.C.17) and (I.C.18) for the lift and moment, involving the operator L_{CK}^{even}. (See, however, Section III.)

In the remainder of this Section we discuss typical results of Scott's calculations as reported in Ref. [8].

B. Airfoil Aerodynamic Response to Imposed Maneuver

A critical part of studying the behavior of wings in maneuver is the understanding of the wing's aerodynamic response to new conditions suddenly imposed. Representative of such response are, for the 2D case, the results of the classical Wagner problem, illustrated for the low-amplitude (linear) case in Figure II.1.a. The net bound circulation on the airfoil ($\Gamma_0 + \Gamma_1$ in the Figure) adjusts only gradually to the suddenly imposed change in angle-of-attack as represented by the jump in Γ_0. The lift coefficient jumps to ½ its eventual value and gradually adjusts. Note that the relaxation to the quasi-steady result is very slow. (On the Figures, time is normalized to $c/4\ U_\infty$).

The corresponding large-amplitude case is illustrated in Figure II.1.c. Qualitatively, the response is very similar to the linearized result, despite the relatively severe deformation of the wake as illustrated in Figure II.1.d. (Compare Figure II.1.b.) This bodes well for the effectiveness of the linear analysis for this type of problem, and is consistent with the fact that the wing in each case is adjusting to vorticity rather strongly concentrated toward the far reaches of the wake.

The response of an airfoil to imposed low-amplitude long-duration oscillatory motion (plunging in this case) is illustrated in Figure II.2 (a through d). Corresponding to classical linear theory, for times long enough after imposition of the motion, the lift either lags or leads the quasi-steady value, depending on the value of the reduced frequency. The results provide a necessary check of the present non-linear method. (The wakes are not shown in these particular examples, as they were negligibly displaced or wrinkled.)

The values of lead or lag indicated in Figure II.2 are generally small. They also agree only qualitatively with the classical linear theory. This fact provided us with the first indication of certain numerical inaccuracies arising from the use of (I.C.17) and (I.C.18). The remedy is discussed in Section III. (See also the remarks at the end of Section I.C.)

Illustration of the airfoil's aerodynamic response to a rudimentary but severe maneuver is illustrated in Figure II.3. There, a sudden single-cycle sinusoidal angle-of-attack variation of 2° amplitude is imposed and just as suddenly stopped. The wake vorticity coagulates and begins roll-up without significant net displacement from the plane of the airfoil (Figure II.3a). The lift jumps immediately due to the abrupt change in $\dot{\alpha}$ (see Eq. I.B.4) and then <u>leads</u> the quasi-steady value into the

negative lift region. It then overshoots the recovery (because of wake induction), plunges again, and only very slowly recovers to the state before the maneuver. During the maneuver, from start to finish, the airfoil advances 5 chord lengths in this example. Both "apparent mass" effects and upwash induced by the wake play vital roles in the net result.

In all the examples the pitching moment has also been studied and behaves in the classical manner at low amplitudes such as used in Figure II.2. For this sudden, high-amplitude maneuver, however, its behavior, though also classical, emphasizes the need for skilled control responses on the part of the pilot.

Many additional examples are available in the recently-completed thesis of M.T. Scott [8].

III. Planned Improvements of NLWAKE

As mentioned in Section II and anticipated at the end of Section I.C., numerical inaccuracies arise in the use of (I.C.17) and (I.C.18) because of near cancellation between two major wake terms in each of those expressions. Therefore, reformulation of the lift expression, via wake integrals [6] can be very advantageous for numerical purposes. In the following, we discuss some of the steps needed for this purpose in the non-linear treatment.

We begin by focusing on the particular term (see Eq. (I.C.17))

$$\Delta L = (\Delta L_0 + \Delta L_w) \equiv \frac{-\rho_\infty c^2/4}{\cos\alpha} \frac{d}{dt} \int_0^\pi d\beta \sin\beta \cos\beta \, (\Delta \hat{u}_0 + \Delta \hat{u}_w) \qquad \text{(III.1)}$$

where $\Delta \hat{u} = \Delta \hat{u}_0 + \Delta u_w$ is given in (I.C.9) and $\Delta \hat{u}_0$ is the "quasi-steady" form

$$\Delta \hat{u}_0 = \left(\frac{1-\cos\beta}{\sin\beta}\right)\left(2 U_\infty \sin\alpha - 2 \dot{h} \cos\alpha + 2 \hat{x}\dot{\alpha}\right) \qquad \text{(III.2)}$$

and

$$\Delta \hat{u}_w = \frac{+L_{CK}^{even}(\beta) \{2 \sin\tau \hat{v}_w(\tau,t)\}}{\sin\beta} \qquad \text{(III.3)}$$

as defined in Section I.C. We recognize ΔL_0 as the classical "apparent mass" contribution [6] involving only quasi-steady terms.

But ΔL_w can be re-expressed in terms of an integral over the wake vorticity, using the Biot Savart Law and Eqs. (II.1) - (II.4). The result is

$$\Delta L_w = \frac{\rho_\infty c/2}{\cos\alpha} \frac{d}{dt} \left\{ \text{Real Part} \left(-\int_t^0 d\lambda \frac{d\Gamma_w}{d\lambda}(\lambda) \left[\sqrt{a^2-1} - a\right] \right) \right\} \qquad \text{(III.4)}$$

with "a" defined as in Eq. (II.1).

Similarly, if we focus on the contribution

$$\Delta L^1 \equiv \Delta L_0^1 + \Delta L_w^1 = \frac{\rho_\infty (c/2)^2}{\cos\alpha} \frac{d}{dt} \int_0^\pi d\beta \sin\beta \, (\Delta \hat{u}_0 + \Delta \hat{u}_w) \qquad \text{(III.5)}$$

we see that

$$\Delta L_0^1 = -\frac{\rho_\infty c/2}{\cos\alpha} \frac{d\Gamma_0}{dt} \qquad \text{(III.6)}$$

and

$$\Delta L_w^1 = \frac{-\rho_\infty c/2}{\cos\alpha} \frac{d\Gamma_1}{dt} \tag{III.7}$$

so that

$$\Delta L^1 = \frac{-\rho_\infty c/2}{\cos\alpha} \frac{d\Gamma_{Bound}}{dt} .$$

Going further, we perform the time derivative in (III.4), to obtain

$$\Delta L_w = \frac{-\rho_\infty c/2}{\cos\alpha} \frac{d\Gamma_{wake}}{dt} - \frac{\rho_\infty c/2}{\cos\alpha} \int_t^0 d\lambda \frac{d\Gamma_w}{d\lambda} \frac{\partial a(\lambda,t)}{\partial t} \left\{ \frac{a}{\sqrt{a^2-1}} - 1 \right\} \tag{III.8}$$

Thus, since $\Gamma_{wake} = -\Gamma_{Bound}$, some exact cancellations occur* and we find, following Kármán and Sears,

$$\Delta L_0 + \Delta L_w + \Delta L_w^1 + \Delta L_0^1 =$$

$$= \Delta L_0(t) + L_2(t) + L_3(t) \tag{III.9}$$

"apparent mass" "wake effect" "$\rho U_\infty \Gamma_1$ + non-linear correction"

where ΔL_0 has its exact classical form [6], and

$$L_2 \equiv \frac{+\rho_\infty c/2}{\cos\alpha} \int_t^0 d\lambda \frac{d\Gamma_w}{d\lambda} \frac{\partial a(\lambda,t)}{\partial t} \frac{1}{\sqrt{a^2-1}} \tag{III.10}$$

$$L_3 \equiv \rho_\infty U_\infty \Gamma_1 - \frac{\rho_\infty}{\cos\alpha} \int_t^0 d\lambda \frac{d\Gamma_w}{d\lambda} \left(\frac{c}{2} \frac{\partial a}{\partial t} - U_\infty \cos\alpha \right) \left[\sqrt{\frac{a+1}{a-1}} - 1 \right] \tag{III.11.}$$

In (III.11) we have used (II.4) to eliminate $\Gamma_1(t)$. Note that in the low-amplitude limit $\frac{c}{2} \frac{\partial a}{\partial t} \to U_\infty$ and $\cos\alpha \to 1$, so the second term in (III.11) vanishes exactly in linearized theory.

Finally, we note the $\rho_\infty U_\infty \Gamma_1$ term in (III.11) exactly cancels the leading term in (I.C.19). Thus, reformulation of the lift expression allows total elimination of "$\rho_\infty U_\infty \Gamma_1$", just as in [6]. In the final expression for the lift the only terms proportional to Γ_1 are non-linear in origin, and the lift expression

*For example, in the final net expression for lift, no terms proportional to either $\frac{d\Gamma_1}{dt}$ or $\frac{d\Gamma_0}{dt}$ occur.

reduces exactly to the classical result in the limit of low amplitudes airfoil motion. The computational advantages of this approach are clear and are being exploited in advanced versions of NLWAKE. Similar results for the moment are also to be used.

References

1. McCune, J.E., "A Proposed Study of the High-Angle-of-Attack Aerodynamics of a Slender Delta Wing." Internal Report, M.I.T., May 1985.

2. Jones, R.T., "Properties of Low-Aspect-Ratio Pointed Wings at Speeds Below and Above the Speed of Sound." NACA Report 835.

3. Rott, N., "Vortices." The 3rd Annual W.R. Sears Distinguished Lecture, Cornell University, April 30, 1987.

4. Mook, D.T., et. al. "On the Numerical Simulation of the Unsteady Wake Behind an Airfoil." AIAA-87-0190, Engineering Science and Mechanics Department, Virginia Polytechnic Institute and State University.

5. Wagner, H., "Dynamischer Auftrieb von Tragflügeln." Z.A.M.M. 5, 1925.

6. Karman, Th. von, and Sears, W.R., "Airfoil Theory for Non-Uniform Motion." J. Aeron. Sci., 5, 1938.

7. Theodorsen, Th., "General Theory of Aerodynamic Instability and the Mechanism of Flutter." NACA Report 496.

8. Scott, M., "Non-linear Airfoil Wake Interaction in Large Amplitude Unsteady Flow." M.I.T., M.S. Thesis, June, 1987.

9. Munk, M., "The Aerodynamic Forces of Airship Hulls." NACA Report 184.

10. Ashley, H., and Landahl, M., Aerodynamics of Wings and Bodies, Addison-Wesley, 1965.

11. Adams, Mac, "Leading-Edge Separation from Delta Wings at Supersonic Speeds." J. Aeron. Sci., 20, Reader's Forum, June, 1953.

12. Edwards, R.H., "Leading-Edge Separation from Delta Wings." J. Aeron. Sci., 21, Reader's Forum, Nov., 1953.

13. Cheng, H.K., "Remarks on Non-linear Lift and Vortex Separation." J. Aeron. Sci., 21, Reader's Forum, Dec., 1953.

14. Brown, C.E., and Michael, W.H., Jr., "Effect of Leading-Edge Separation on the Lift of a Delta Wing," J. Aeron. Sci., 21, 1953.

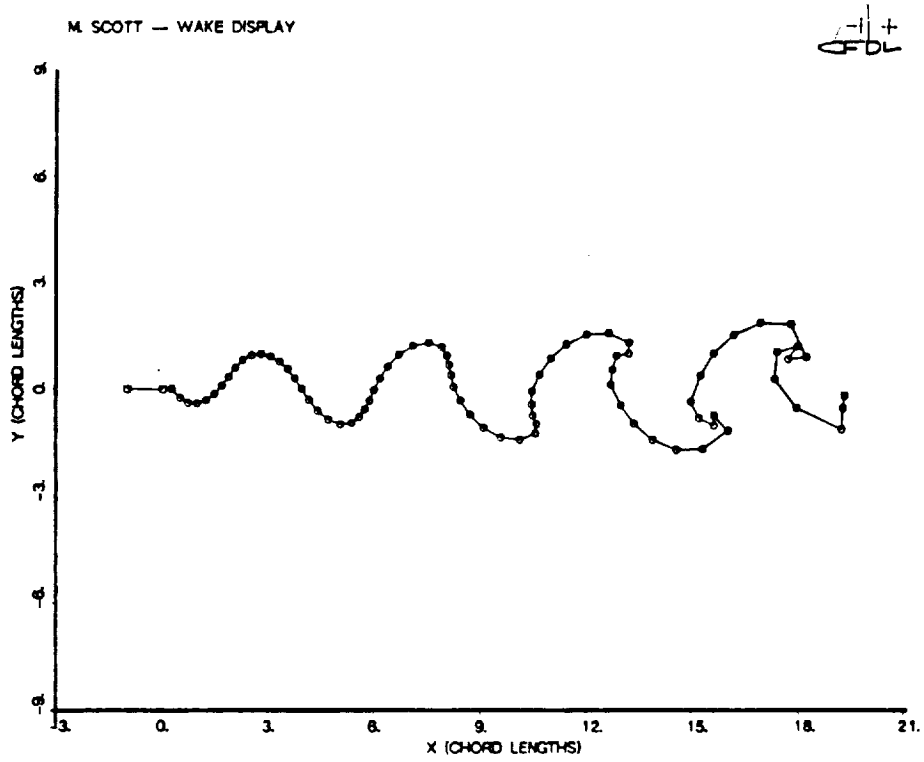

Figure I.1 Wake behind an oscillating airfoil.

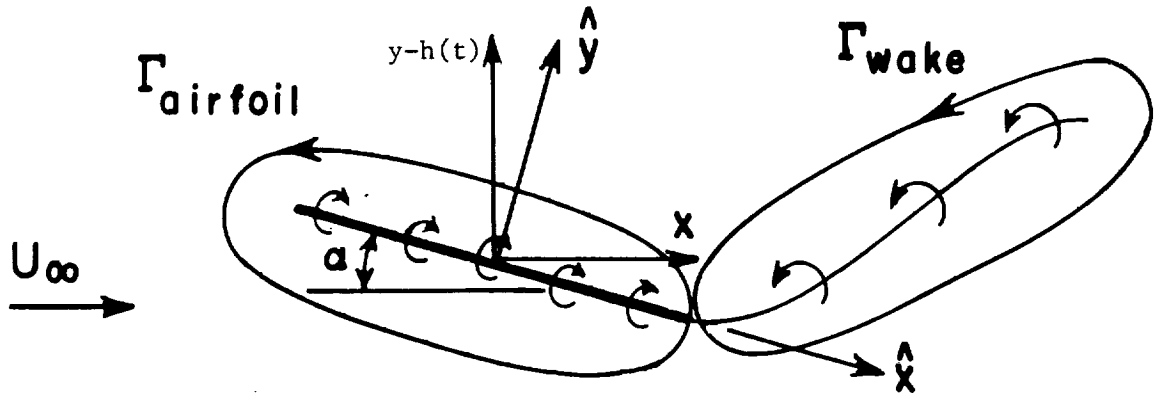

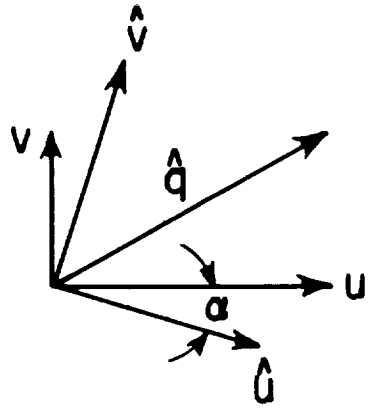

q̂ = Velocity Vector

Figure I.2 Instantaneous coordinate system $(\hat{x},\hat{y})$ fixed in oscillating plate.

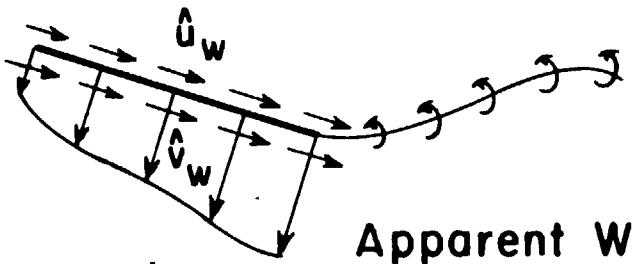

Apparent Wake Induced Velocity

+

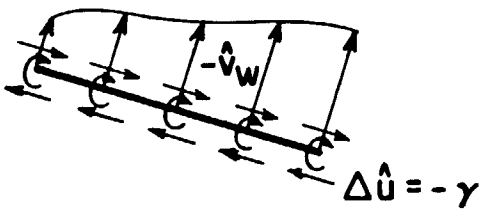

= Velocity Due To Additional Bound Vorticity

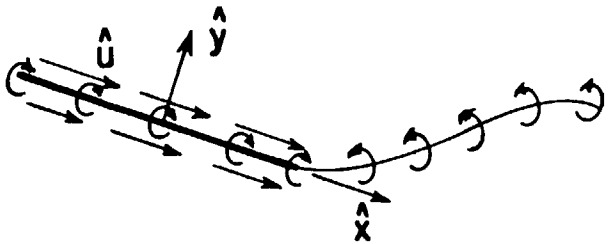

Net Flow With Normal Velocity Cancelled At Airfoil Surface

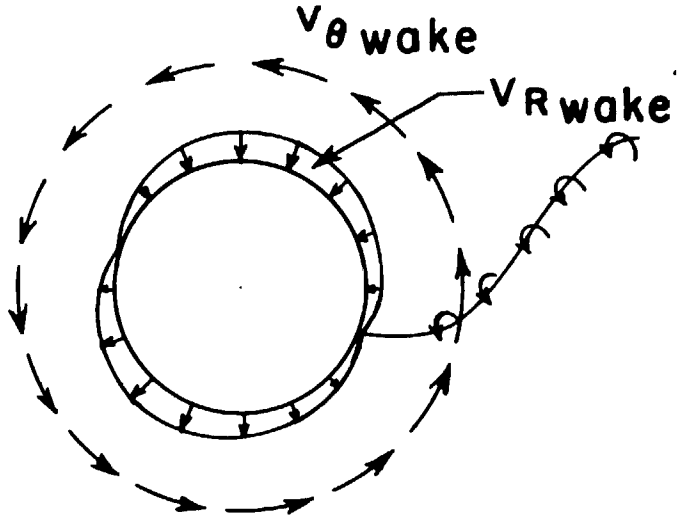

Radial And Tangential Components Of Wake Induced Velocity As Viewed In The Circle Plane

Figure I.3 Superposition Algorithm for determining bound vorticity necessary to cancel wake upwash at the plate.

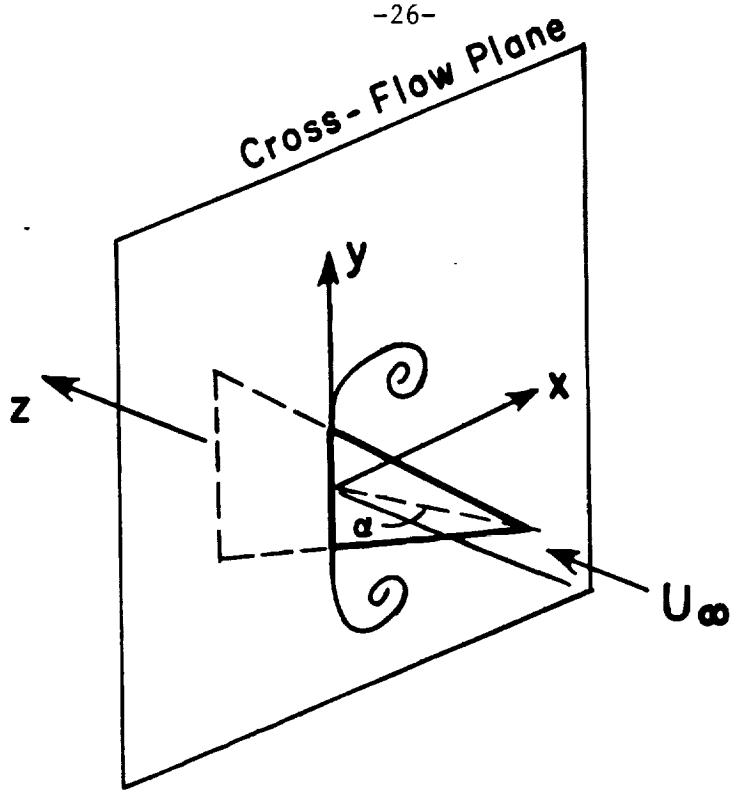

a) Penetration Of Delta Wing Through Fixed Reference Cross-Plane

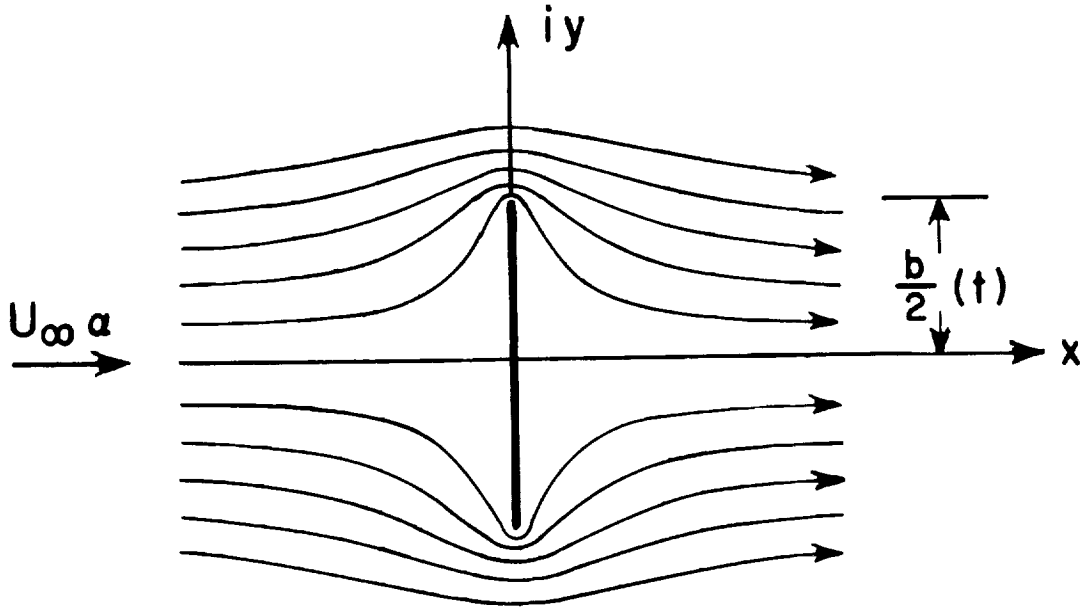

b) Streamlines Of The Cross-Flow Without Enforcing Kutta Condition

Figure I.4 a) Time analogy. b) Cross-plane flow configuration, singular at wing edges when no "wake" is present.

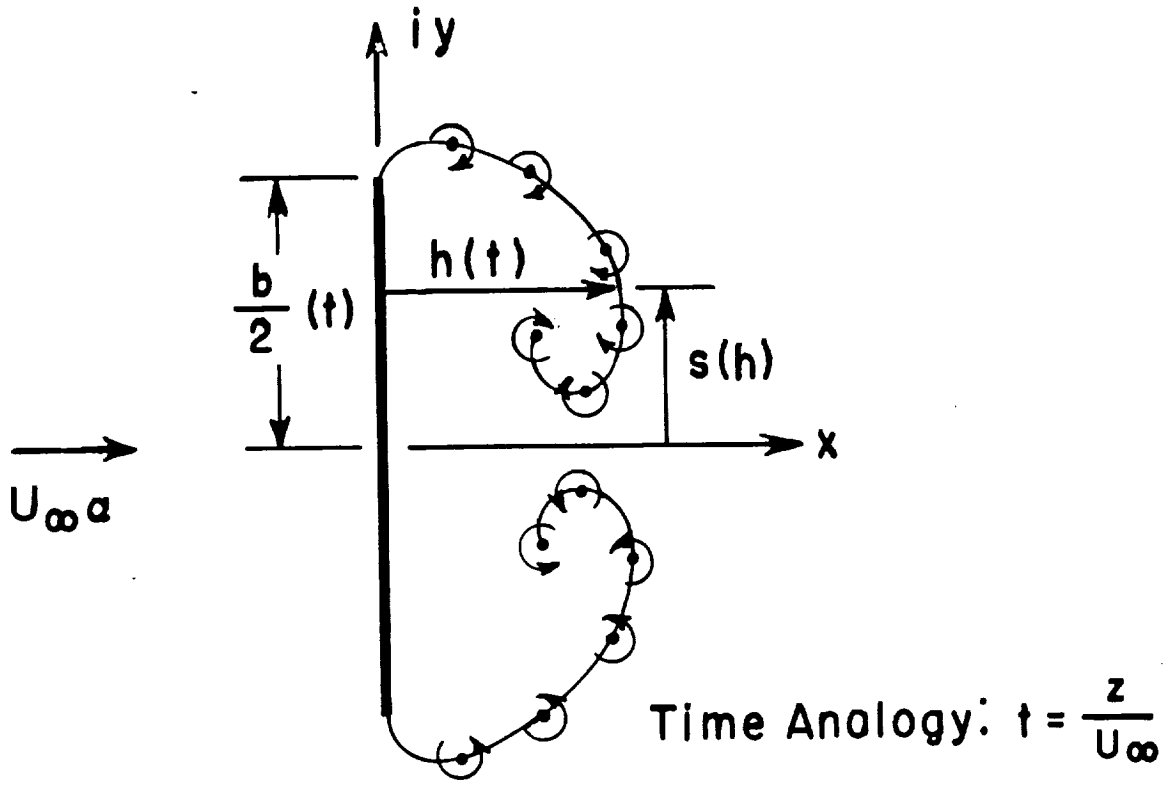

a) Non-Linear Representation Of Wakes

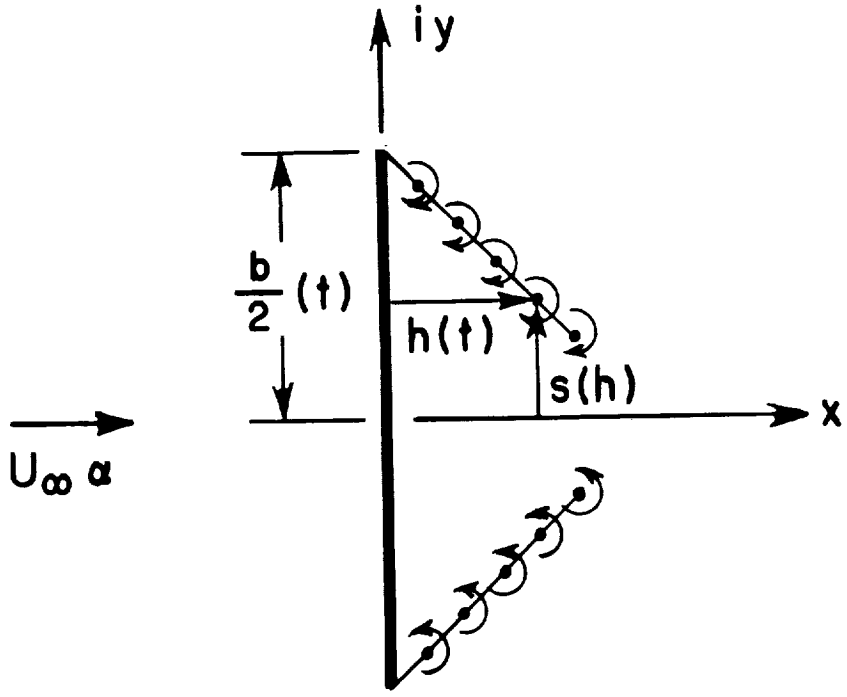

b) Linear Representation Of Wakes

Figure I.5 Wake configuration leading to satisfaction of Kutta condition at wing edges in each cross-plane.

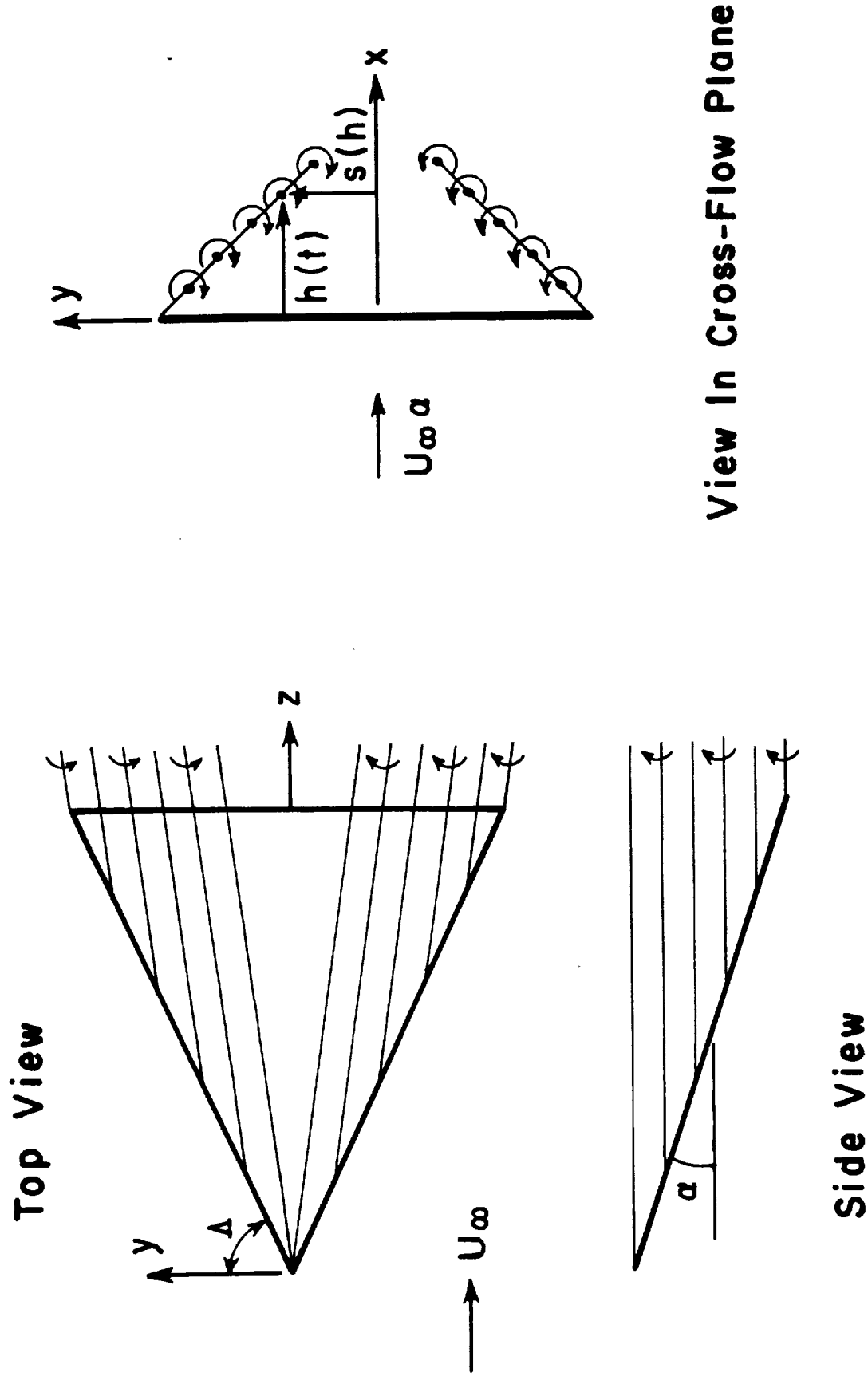

Figure I.6 Linearized version of leading edge separation and wake trace formation.

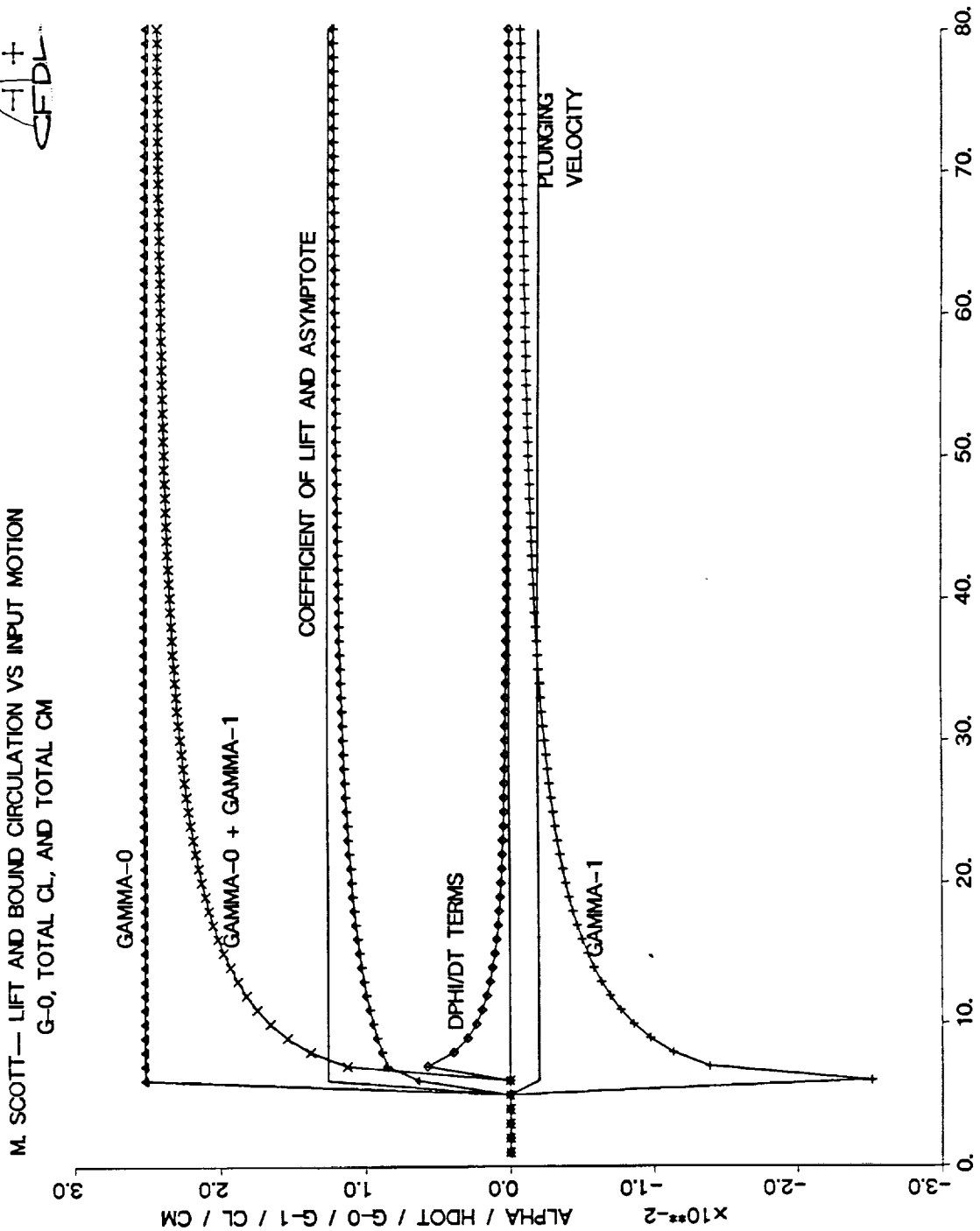

Figure II.1.a Low amplitude step in plunging velocity.
$|\hat{h}| = .002\ U_\infty$. Step imposed at t=5.
Unit of time = $c/4\ U_\infty$.

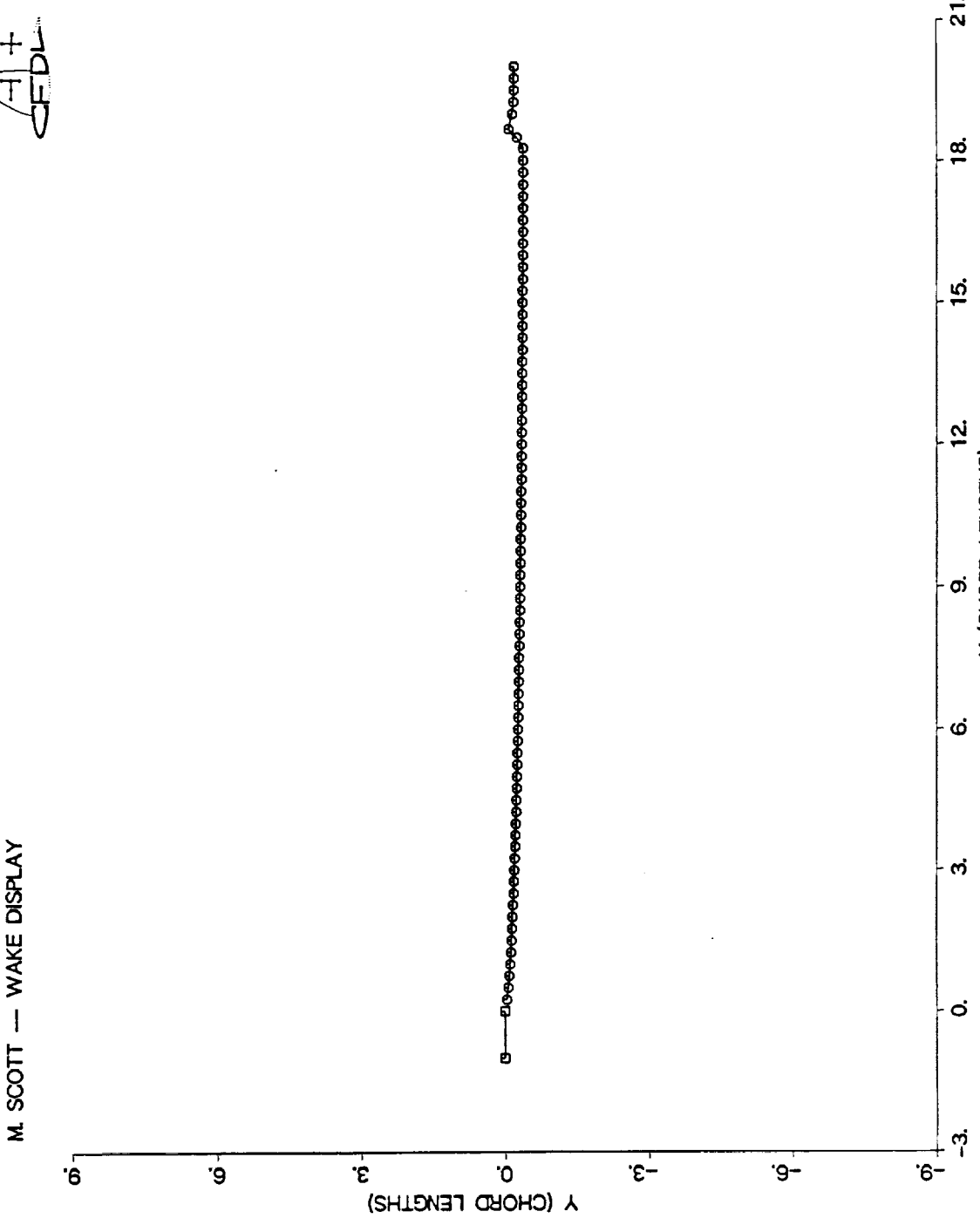

Figure II.1.b Wake for the low amplitude "step" depicted after airfoil has travelled 20 chord lengths.

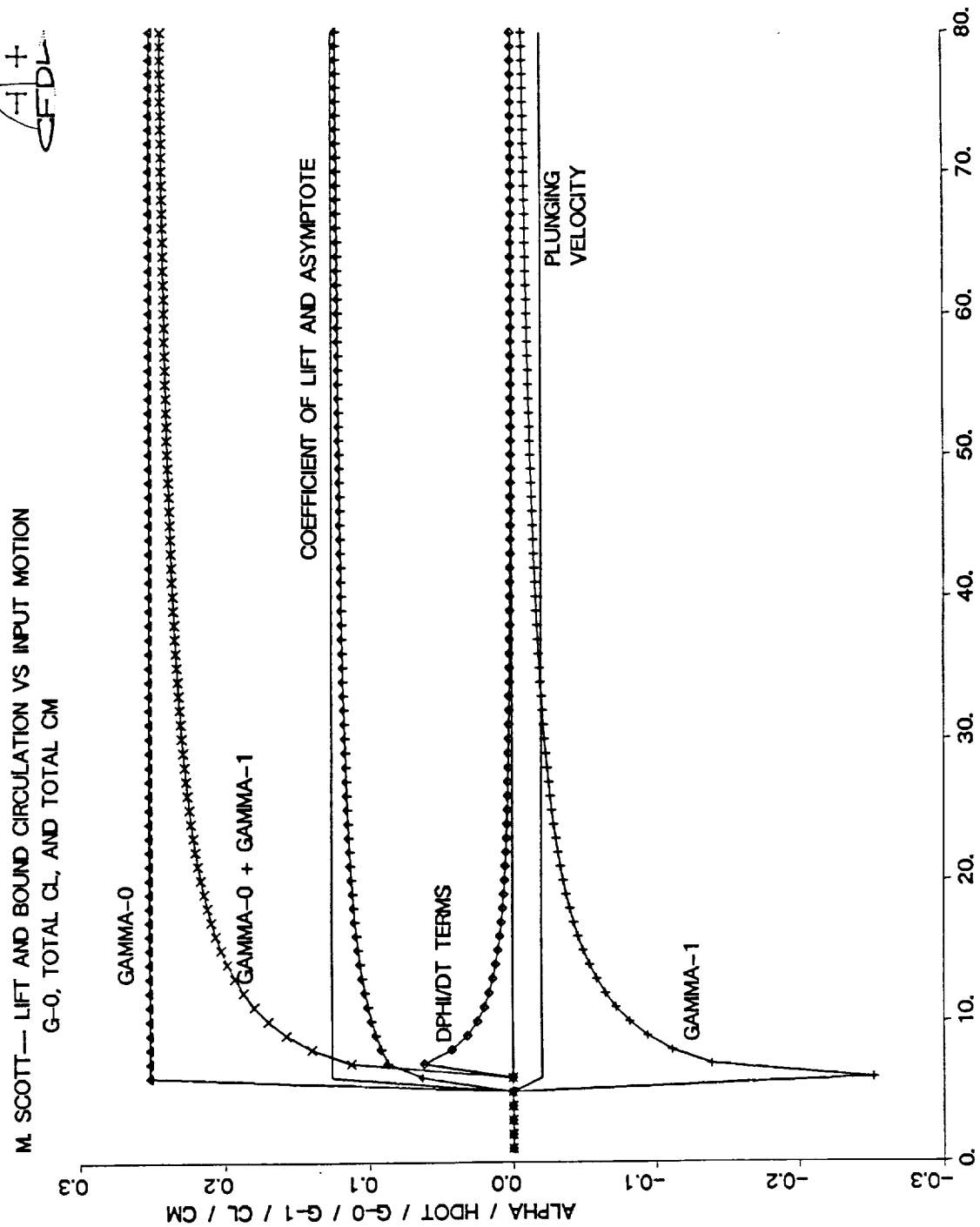

Figure II.1.c Large amplitude step in plunge velocity.
$|\dot{h}| = .02\ U_\infty$. Step imposed at t=5.
Unit of time = c/4 U_∞.

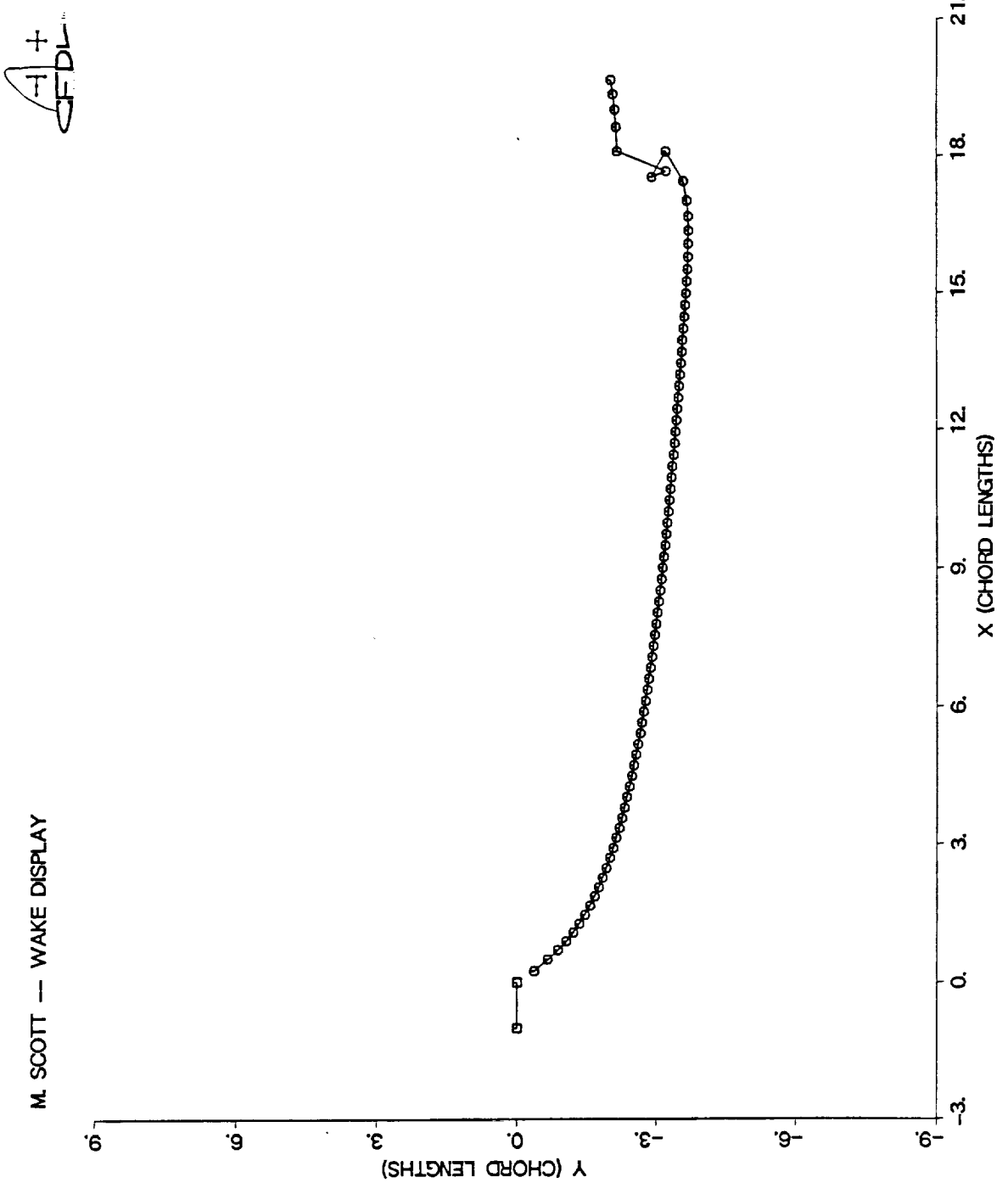

Figure II.1.d Wake for the high-amplitude "step" depicted after airfoil has travelled 20 chord lengths.

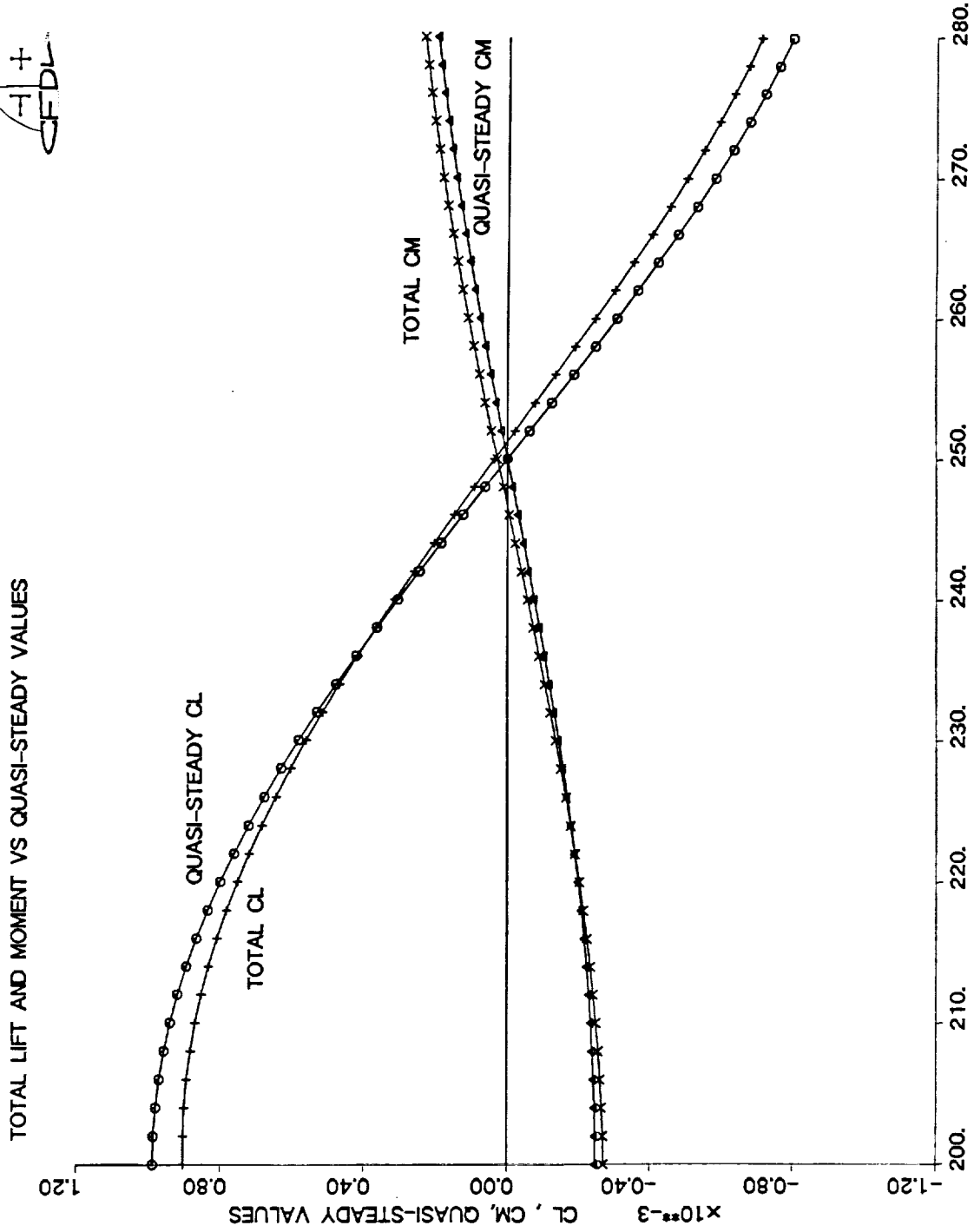

Figure II.2.a Low amplitude plunging oscillation at a reduced frequency, f=.005.

Here $f = \frac{w(\text{cycles/time})c}{4\,U_\infty}$. Lift lags by 2.26°. $h=h_0 \sin(2\pi ft)$.

h_0=.005 quarter chords.

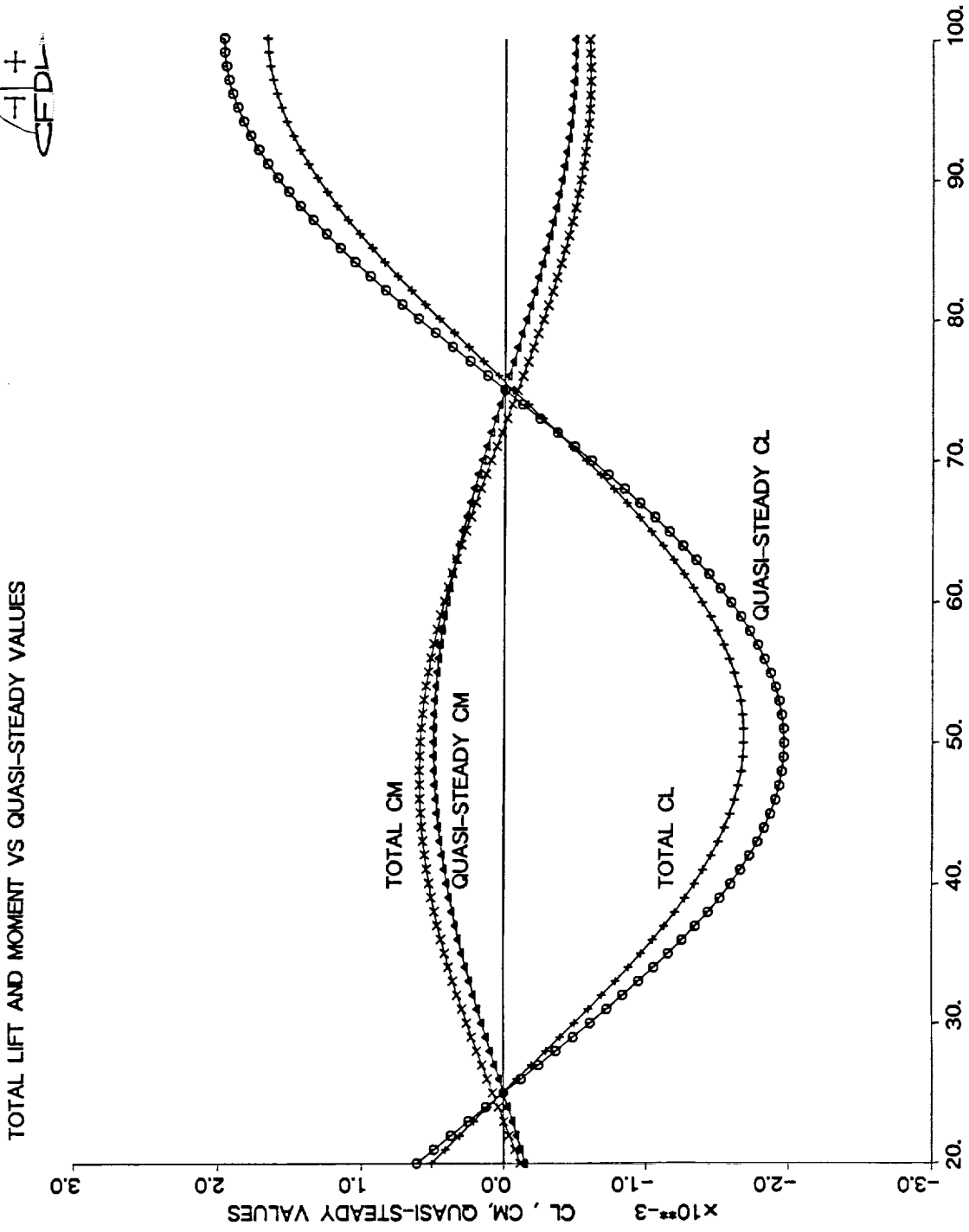

Figure II.2.b Same as II.2.a except f=.01. Lift lags by 1.8°.

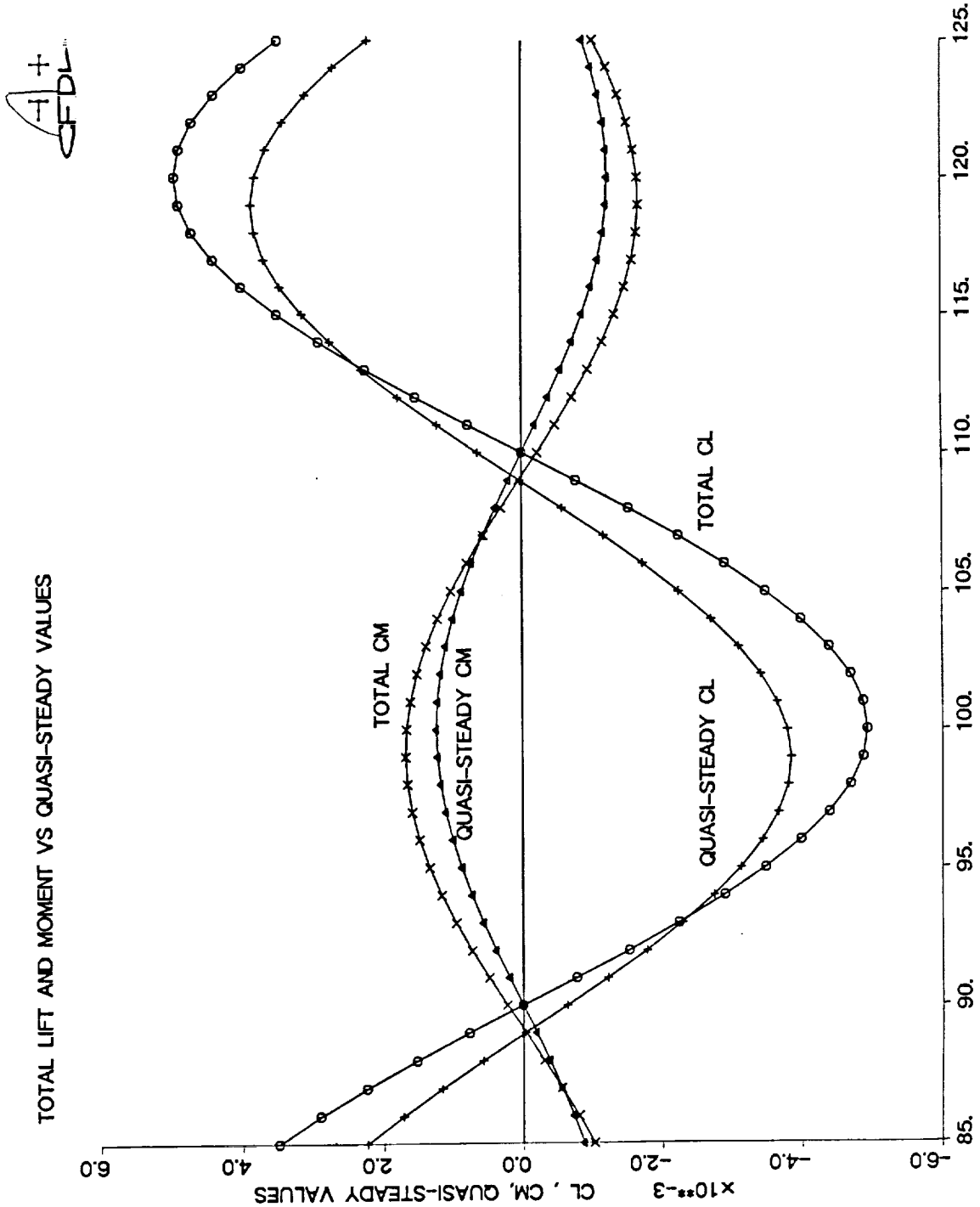

Figure II.2.c Same as II.2.a except f=.025. Lift leads by 7.8°.

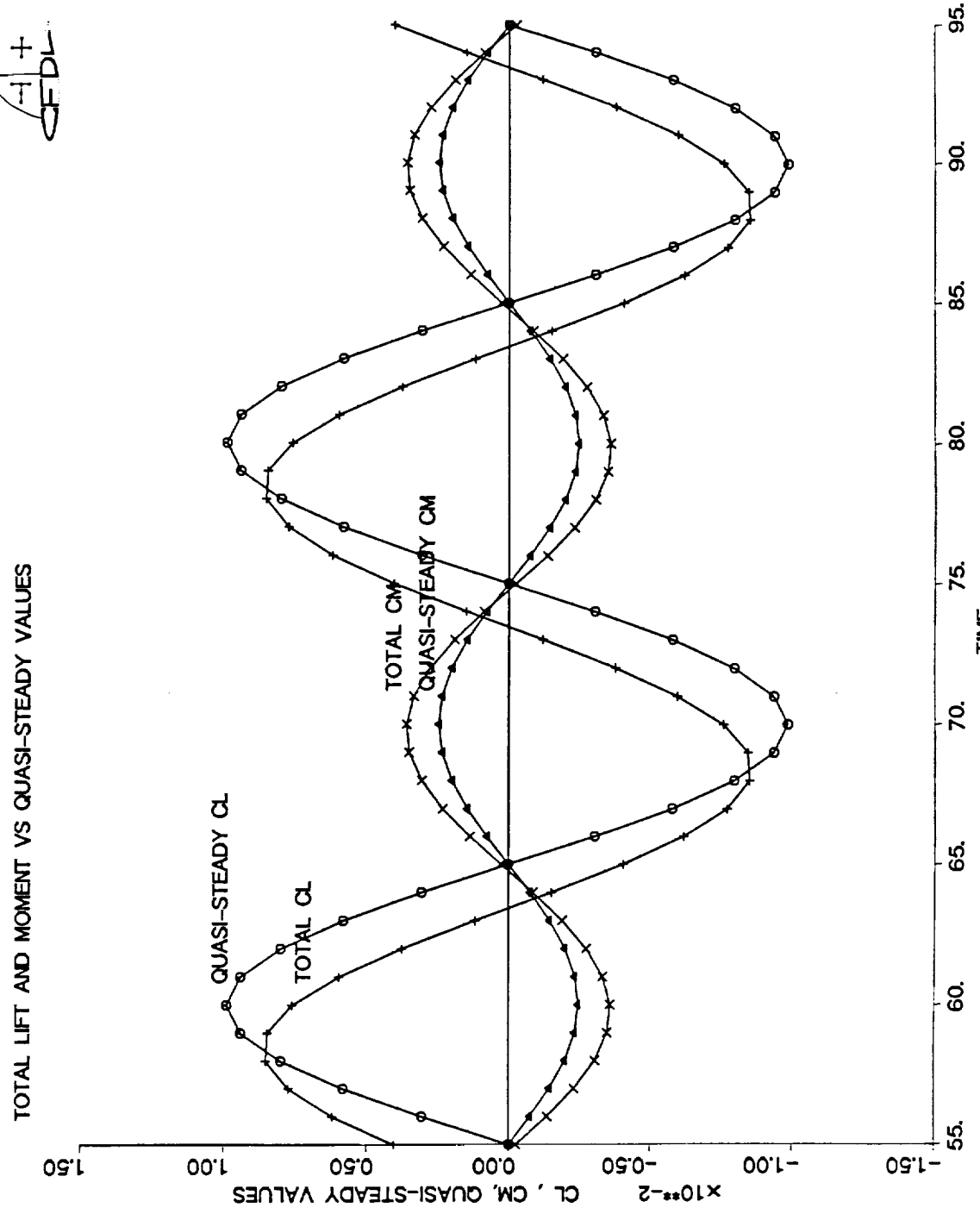

Figure II.2.d Same as II.2.a except f=.05. Lift leads by 28°.

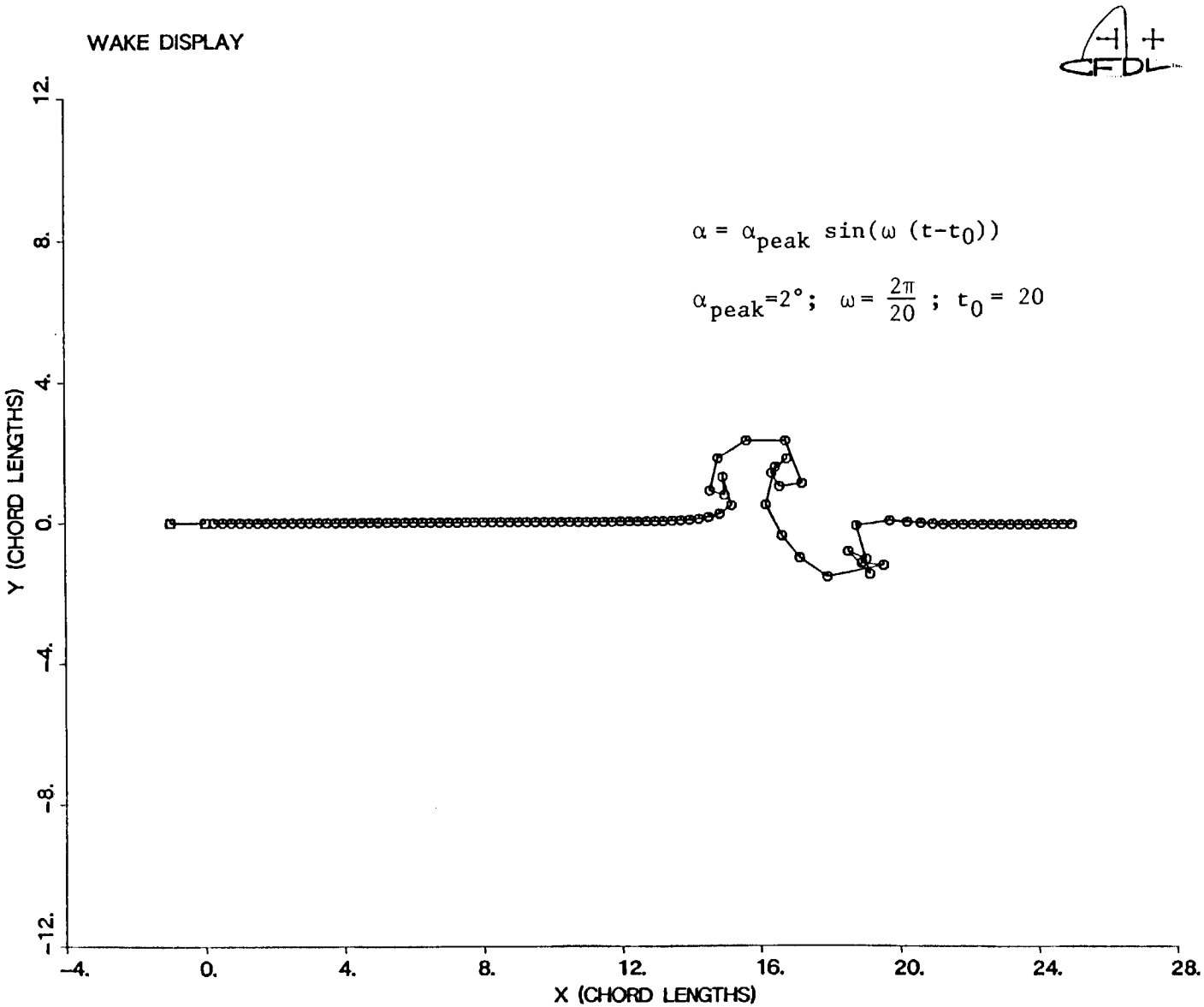

Figure II.3.a Wake structure after a 5-chord length severe sinusoid maneuver. (See also Fig. II.3.b) Wake depicted after airfoil has moved an additional twelve chord lengths after the end of the maneuver.

t_0=5; t_{end}= 10. Units of t are c/4 U_∞.

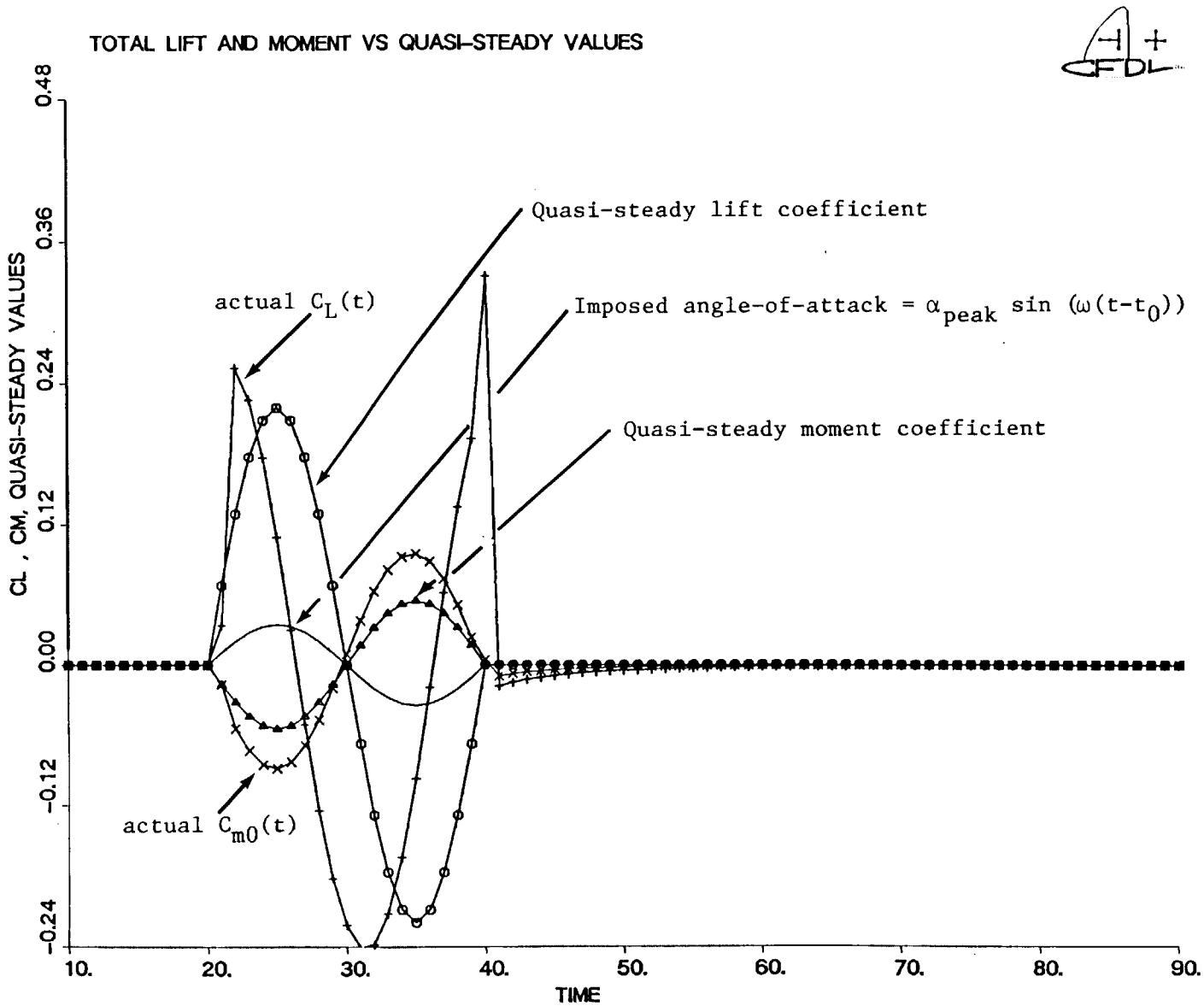

Figure II.3.b Lift and moment response to the severe 5-chord length sinusoid maneuver of Fig. II.3.a. Peak angle of attack change 2°.